Journal of Solid State Chemistry **163,** 513–518 (2002)
doi:10.1006/jssc.2001.9439 available online at http://www.idealibrary.com on IDEAL®

Magnetic Susceptibility and Spin Exchange Interactions of the Hexagonal Perovskite-Type Oxides $Sr_{4/3}(Mn_{2/3}Ni_{1/3})O_3$

A. El Abed,*,† E. Gaudin,* J. Darriet,*,[1] and M.-H. Whangbo‡,[1]

*Institut de Chimie de la Matière Condensée de Bordeaux (ICMCB UPR 9048 CNRS), 87 Avenue du Dr. A. Schweitzer, 33608 Pessac Cedex, France; †Laboratoire de Physique du Solide, Faculté des Sciences, Université Mohamed 1er, Oujda, Morocco; and ‡Department of Chemistry, North Carolina State University, Raleigh, North Carolina 27695-8204

Received July 24, 2001; in revised form October 8, 2001; accepted October 26, 2001

Magnetic susceptibility measurements were carried out for two hexagonal perovskite-type oxides $Sr_{1+x}(Mn_{1-x}Ni_x)O_3$ with slightly different compositions (i.e., $x = \frac{1}{3}$ and 0.324). A significant difference in the susceptibilities of the two phases demonstrates the need to control phase compositions accurately. $Sr_{4/3}(Mn_{2/3}Ni_{1/3})O_3$ consists of two spin sublattices, i.e., the Mn^{4+} and the Ni^{2+} ion sublattices. Spin dimer analysis was carried out to examine the relative strengths in the spin exchange interactions of the Mn^{4+} ion sublattice. The temperature dependence of the magnetic susceptibility of $Sr_{4/3}(Mn_{2/3}Ni_{1/3})O_3$ was found consistent with a picture in which the Mn^{4+} ion sublattice has weakly interacting antiferromagnetically coupled $(Mn^{4+})_2$ dimers, the Ni^{2+} ion sublattice acts as a paramagnetic system, and the two sublattices are nearly independent. © 2002 Elsevier Science (USA)

1. INTRODUCTION

In recent years the structures and magnetic properties of hexagonal perovskite-type oxides A_xMO_3 ($x = \frac{6}{5}, \frac{9}{7}, \frac{14}{11}$; $A = Sr$, Ba; $M = Co$, Ni) have received much attention (1–6). The structures of these oxides can be viewed in terms of infinite $(MO_3)_\infty$ and A_∞ chains (Fig. 1), where the $(MO_3)_\infty$ chains are made up of face-sharing MO_6 octahedra and trigonal prisms. In the $(MO_3)_\infty$ chains, single MO_6 trigonal prisms may alternate with single MO_6 octahedra (1) or with M_nO_{3n+3} octahedral oligomers made up of n face-sharing MO_6 octahedra (2–6) (Fig. 2). In the infinite $(MO_3)_\infty$ chains of the incommensurate phase $Sr_{1.2872}NiO_3$ (7), which is approximated by the commensurate structure $Sr_{9/7}NiO_3$, the MO_6 trigonal prisms alternate randomly with two types of octahedral oligomers M_2O_9 and M_3O_{12}. Analysis of the M–O bond lengths in $Sr_{14/11}CoO_3$ (5) and $Sr_{9/7}NiO_3$ (7) indicates that the oxidation states of the transition metal atoms in the octahedral (Oh) and trigonal prism (TP) MO_6 units are close to $+4$ and $+2$, respectively. Thus, in hexagonal perovskite-type oxides containing two different transition metals, the more electronegative ones should occupy the TP sites. Indeed, the recent study of $Sr_{4/3}(Mn_{2/3}Ni_{1/3})O_3$ (6), whose $(MO_3)_\infty$ chains have Mn_2O_9 octahedral dimers alternate with single NiO_6 trigonal prisms (Fig. 2b), shows that the Oh and TP sites are occupied exclusively by Mn^{4+} (d^3) and Ni^{2+} (d^8) ions, respectively. As found for $Sr_{9/7}NiO_3$ (7), the Ni^{2+} ions of $Sr_{4/3}(Mn_{2/3}Ni_{1/3})O_3$ occupy several different coordination sites of the NiO_6 trigonal prisms. According to the X-ray powder diffraction and XANES studies (6), approximately 80% of the Ni^{2+} ions are located at the three square-planar (SP) coordination sites, and approximately 20% of the Ni^{2+} ions at the TP centers. (A unit cell of $Sr_{4/3}(Mn_{2/3}Ni_{1/3})O_3$ has one $(MO_3)_\infty$ chain consisting of Mn(1) and Ni(1) atoms and two $(MO_3)_\infty$ chains consisting of Mn(2), Mn(3), Ni(2), and Ni(3) atoms. The occupancies of the SP and TP centers are 0.751(4) and 0.249 (4), respectively, in the $(MO_3)_\infty$ chain containing Ni(1) atoms, and 0.829(4) and 0.171(4), respectively, in the $(MO_3)_\infty$ chain containing Ni(2) and Ni(3) atoms.)

The Ni^{2+} ions at the SP centers prefer the $S = 0$ spin state, but those at the TP centers the $S = 1$ spin state (8). The Mn K-edge XANES study (6) of $Sr_{4/3}(Mn_{2/3}Ni_{1/3})O_3$ showed that the Mn^{4+} ions are in a high-spin ($S = \frac{3}{2}$) state. Each Mn^{4+} ion can have spin-exchange interactions with adjacent Mn^{4+} ions and also with adjacent Ni^{2+} ions if the latter are located at the TP centers. Thus, a number of different local spin arrangements are possible in $Sr_{4/3}(Mn_{2/3}Ni_{1/3})O_3$, and one would expect the description of its magnetic properties to be rather complicated. Nevertheless, as will be shown below, the essential features of the magnetic susceptibility of this compound are well described using the simple approximation that the spin exchange interactions between the Mn^{4+} and Ni^{2+} ions are negligible. In the present work, we report the magnetic susceptibilities of two hexagonal perovskite-type oxides Sr_{1+x}

[1]To whom correspondence should be addressed.

0022-4596/02 $35.00

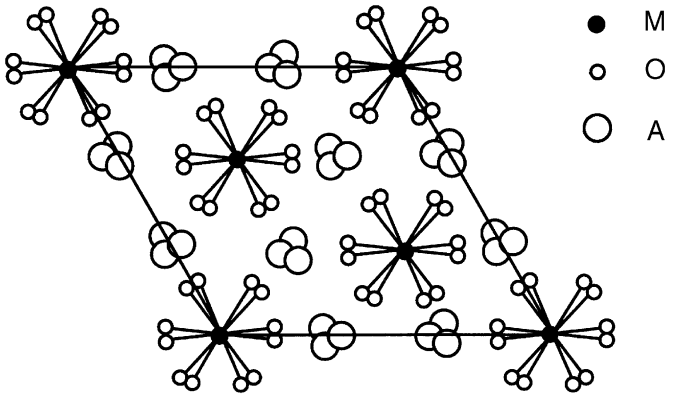

FIG. 1. Schematic projection view of the structure of a hexagonal perovskite-type compound A_xMO_3 along the $(MO_3)_\infty$ chain direction.

$(Mn_{1-x}Ni_x)O_3$ with slightly different compositions (i.e., $x = \frac{1}{3}$ and 0.324). To help understand the magnetic structure of $Sr_{4/3}(Mn_{2/3}Ni_{1/3})O_3$, we estimate the relative strengths of its spin exchange interactions and analyze the temperature dependence of its magnetic susceptibility in some detail.

2. EXPERIMENTAL

As reported earlier (6), the best method to prepare stoichiometric powder samples of $Sr_{1+x}(Mn_{1-x}Ni_x)O_3$ is to fire a stoichiometric mixture of $SrCO_3$, NiO and previously synthesized $Sr_7Mn_4O_{15}$. The mixture is heated at 1200°C for 48 h and reground at frequent intervals. The reaction

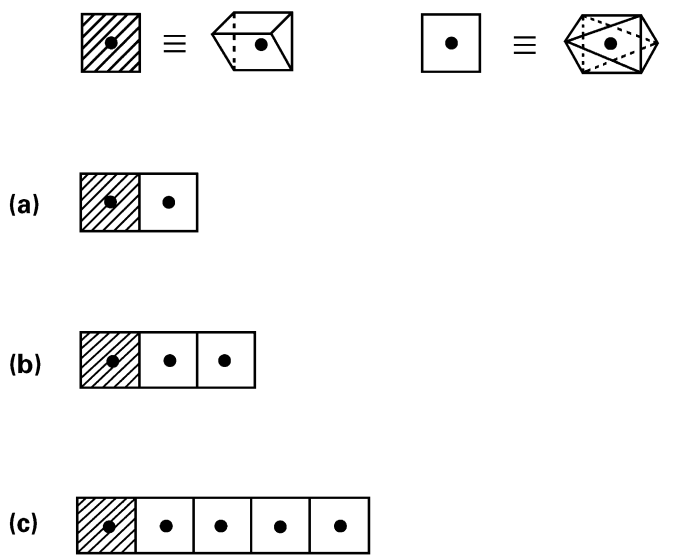

FIG. 2. Schematic representations of the MO_6 octahedra and MO_6 trigonal prisms present in the unit cells of the $(MO_3)_\infty$ chains in (a) $Ca_{3/2}CoO_3$, (b) $Sr_{4/3}(Mn_{2/3}Ni_{1/3})O_3$, and (c) $Ba_{6/5}NiO_3$. The shaded squares represent MO_6 trigonal prisms, and the unshaded squares the MO_6 octahedra.

was controlled by a profile analysis of the X-ray powder diffraction as reported in Ref. (6). $Sr_7Mn_4O_{15}$ (9) was prepared by heating an appropriate stoichiometric mixture of $SrCO_3$ and Mn_2O_3 under oxygen atmosphere at 1200°C for 48 h. As is well known, the preparation of these materials is challenging and requires accurate control of the heat treatment because phases with a small difference in composition have different unit cell parameters. We prepared two $Sr_{1+x}(Mn_{1-x}Ni_x)O_3$ phases with slightly different compositions (i.e., $x = \frac{1}{3}$ and 0.324). The exact values of x were determined by indexing the X-ray powder patterns using the superspace formalism (6). The unit cell parameters for $x = \frac{1}{3}$ and 0.324 are very similar. Namely, $a = 9.5972$ (8) Å, $c_1 = 2.598(1)$ Å, and $c_2 = 3.898(1)$ Å for $x = \frac{1}{3}$, and $a = 9.608(8)$ Å, $c_1 = 2.581(1)$ Å, and $c_2 = 3.899(1)$ Å for $x = 0.324$. Magnetic susceptibility measurements for $Sr_{1+x}(Mn_{1-x}Ni_x)O_3$ were carried out using a Quantum Design SQUID magnetometer. It was confirmed at $T = 2$ K that the magnetization curves determined by zero-field-cooled (ZFC) and field-cooled (FC) measurements (at the operating field 5 kG) show no hysteresis. It was also verified at $T = 2$ K that the magnetization is linear with the field up to 10 kG.

3. CHARACTERISTIC FEATURES OF THE MAGNETIC SUSCEPTIBILITY

Figure 3 shows the magnetic susceptibilities determined for $Sr_{1+x}(Mn_{1-x}Ni_x)O_3$ ($x = \frac{1}{3}$ and 0.324) as a function of temperature. In the entire temperature range the susceptibility is higher for $x = 0.324$ than for $x = \frac{1}{3}$. This is understandable because the $x = 0.324$ phase has more high-spin Mn^{4+} ions (i.e., more unpaired spins) than does the $x = \frac{1}{3}$ phase. As shown in the inset of Fig. 3, a three-dimensional (3D) antiferromagnetic ordering takes place in the $x = \frac{1}{3}$ phase at low temperature (Néel temperature, $T_N = 3$ K), but not in the $x = 0.324$ phase down to 2 K. Thus, a small change in composition has a drastic effect on the Néel temperature, and hence it is necessary to control phase compositions accurately in studying hexagonal perovskite-type oxides A_xMO_3.

Above 150 K the magnetic susceptibility follows a Curie–Weiss law in both $x = \frac{1}{3}$ and $x = 0.324$ phases. A striking feature of the experimental susceptibility curves $\chi_{exp}(T)$ (Fig. 3) is that they both have a plateau in the temperature region between ~ 100 K and ~ 30 K, but this plateau is more pronounced for $x = \frac{1}{3}$. The occurrence of such a plateau can be envisioned if $Sr_{4/3}(Mn_{2/3}Ni_{1/3})O_3$ has a spin sublattice of paramagnetic ions and that of antiferromagnetically coupled spin dimers and if the interaction between the two sublattices is weak. The structure of $Sr_{4/3}(Mn_{2/3}Ni_{1/3})O_3$ suggests that the NiO_6 trigonal prisms having the Ni^{2+} ions at the TP centers are randomly distributed and hence would form a sublattice of paramagnetic

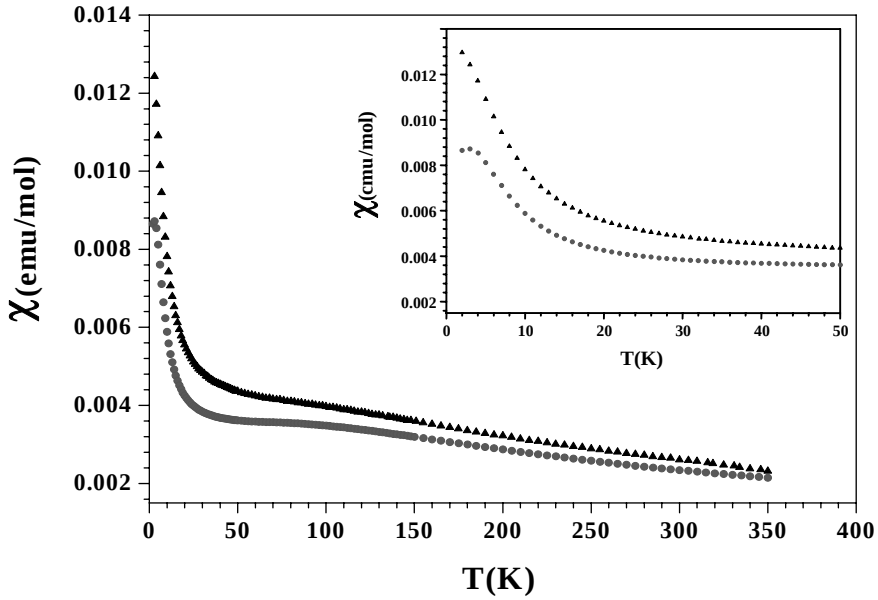

FIG. 3. Magnetic susceptibilities of $Sr_{4/3}(Mn_{2/3}Ni_{1/3})O_3$ (filled circles) and $Sr_{1.324}(Mn_{0.676}Ni_{0.324})O_3$ (filled triangles) as a function of temperature. A zoomed-in view of the susceptibility curves in the low-temperature region is given in the inset.

ions. The Mn_2O_9 octahedral units have an ordered arrangement and would constitute a sublattice of antiferromagnetically coupled $(Mn^{4+})_2$ dimers. In the next section we examine the nature of the spin exchange interactions of the Mn^{4+} ion sublattice in $Sr_{4/3}(Mn_{2/3}Ni_{1/3})O_3$.

4. SPIN EXCHANGE INTERACTIONS

The temperature-dependent magnetic susceptibility of a magnetic solid is described by a spin Hamiltonian, which is expressed in terms of spin exchange parameters J between adjacent spin sites. In principle, the J values of a magnetic solid can be calculated quantitatively by performing electronic structure calculations either for the high- and low-spin states of spin dimers of the magnetic solid (i.e., structural units containing two adjacent spin sites) (10, 11) or for various ordered spin arrangements of the magnetic solid (12). The present work is concerned only with the qualitative trend in the spin exchange interactions of $Sr_{4/3}(Mn_{2/3}Ni_{1/3})O_3$. In general, J is given as a sum of ferromagnetic and antiferromagnetic components, $J = J_F + J_{AF}$.

A spin dimer leads to a superexchange interaction when its two spin sites share common atoms, and to a super-superexchange interaction otherwise (13). Suppose that the two spin sites of a spin dimer are represented by nonorthogonal magnetic orbitals (i.e., singly occupied molecular or bitals of the spin monomers) ϕ_1 and ϕ_2. The antiferromagnetic term is then expressed as $J_{AF} \propto -S_{12}\Delta e$, where S_{12} is the overlap integral between ϕ_1 and ϕ_2, and Δe is the energy separation between the highest two singly occupied energy levels of a spin dimer (Fig. 4) (14, 15). $J_{AF} \propto -(\Delta e)^2$ due to the relationship $\Delta e \propto S_{12}$. The ferromagnetic term is expressed as $J_F \propto K_{12}$, where K_{12} is the exchange repulsion between the two magnetic orbitals, i.e., the Coulomb repulsion resulting from the overlap electron density distribution $\phi_1\phi_2$ (15). A magnetic orbital of a transition metal atom coordinated with oxygen atoms has "oxygen p-orbital tails," which are combined out-of-phase with the transition metal

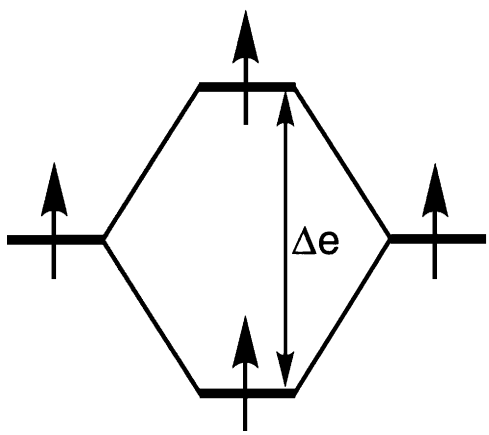

FIG. 4. Spin orbital interaction energy Δe of a spin dimer that is made up of two equivalent spin sites. The magnetic orbitals of the two spin sites interact to produce the two singly filled levels of a spin dimer.

d orbital, and the overlap integral and the overlap electron density between magnetic orbitals are largely determined by their *p*-orbital tails (13, 15). The overlap electron density, and hence the ferromagnetic interaction, should be negligible for a super-superexchange path (M–O $\cdots$ O–M) but can be substantial for a superexchange path (M–O–M) if both magnetic orbitals have large oxygen tails on the same shared oxygen atoms.

When the two adjacent spin sites have m and n unpaired spins, respectively, the trends in the antiferromagnetic spin exchange parameters can be discussed in terms of the average quantities of the spin orbital interaction energies:

$$\langle \Delta e \rangle = \sum_{\mu=1}^{m} \sum_{\nu=1}^{n} \frac{\Delta e_{\mu\nu}}{mn}. \qquad [1a]$$

From the viewpoint of nonorthogonal magnetic orbitals localized at the spin sites, the antiferromagnetic contribution from each term $\Delta e_{\mu\nu}$ is zero (negligible) if the overlap integral $S_{\mu\nu}$ between two adjacent magnetic orbitals is zero by symmetry (negligibly small due to orbital mismatch). Thus, for $m = n$, Eq. [1b] is simplified as (16)

$$\langle \Delta e \rangle \approx \sum_{\mu=1}^{m} \frac{\Delta e_{\mu\mu}}{m^2}. \qquad [1b]$$

Qualitative trends in spin exchange interactions of various magnetic solids are well explained by the $\langle \Delta e \rangle$ values of their spin dimers obtained by extended Hückel calculations (13, 16), which are employed in the present study. In $Sr_{4/3}(Mn_{2/3}Ni_{1/3})O_3$, the Mn^{4+} ion sublattice has an ordered arrangement of spin sites, but the Ni^{2+} ion sublattice does not because the TP centers having Ni^{2+} cations are randomly distributed. There are several pathways for the spin exchange interactions between adjacent Mn^{4+} ions in $Sr_{4/3}(Mn_{2/3}Ni_{1/3})O_3$, namely, the intradimer interaction within each $(MO_3)_\infty$ chain (i.e., intrachain interdimer interaction) and that between adjacent $(MO_3)_\infty$ chains (i.e., interchain interdimer interaction). The spin monomers of $Sr_{4/3}(Mn_{2/3}Ni_{1/3})O_3$ containing the Mn^{4+} ions are the $(MnO_6)^{8-}$ octahedra. The three unpaired spins of each $(MnO_6)^{8-}$ octahedron are accommodated in the t_{2g} levels. The spin dimer for the intradimer interaction is the $(Mn_2O_9)^{10-}$ cluster, and that for the interdimer interaction is the $(Mn_2O_{12})^{16-}$ cluster made up of two isolated $(MnO_6)^{8-}$ octahedra. Our calculations show that the $\langle \Delta e \rangle$ values are considerably larger for the intra-dimer interaction than for the intrachain interdimer interaction [e.g., 56 vs 7 meV for the $(MO_3)_\infty$ chain containing the Mn(1) and Ni(1) atoms]. The $\langle \Delta e \rangle$ value for an interchain interdimer interaction is negligible compared with that for the intrachain interdimer interaction.

5. TWO-INDEPENDENT-SPIN SUBLATTICE MODEL AND ITS IMPLICATIONS

In the Mn^{4+} ion sublattice of $Sr_{4/3}(Mn_{2/3}Ni_{1/3})O_3$ the spin exchange interaction is strongest within each $(Mn^{4+})_2$ dimer and weak interactions between adjacent $(Mn^{4+})_2$ dimers occur mainly in each $(MO_3)_\infty$ chain. The Ni^{2+} ion sublattice of $Sr_{4/3}(Mn_{2/3}Ni_{1/3})O_3$ has no ordered arrangement of spin centers. To a first approximation, we consider $Sr_{4/3}(Mn_{2/3}Ni_{1/3})O_3$ as a spin system in which the Ni^{2+} ion spin sublattice does not interact with the Mn^{4+} ion spin sublattice consisting of weakly interacting antiferromagnetically coupled $(Mn^{4+})_2$ dimers. The calculated susceptibility curve, $\chi_{calc}(T)$, expected for this "two-independent-spin lattice" (TISS) model can be written as

$$\chi_{calc}(T) = \tfrac{1}{3}[y\chi_d(T) + (1 - y)\chi_p(T)], \qquad [2]$$

where y refers to the mole fractions of the $(Mn^{4+})_2$ dimers, and $(1 - y)$ to that of the Ni^{2+} ions located at the TP centers. The susceptibility $\chi_d(T)$ of the Mn^{4+} ion sublattice is normalized to one $(Mn^{4+})_2$ dimer, the susceptibility $\chi_p(T)$ of the Ni^{2+} ion sublattice to one Ni^{2+} cation, and the susceptibilities $\chi_{calc}(T)$ and $\chi_{exp}(T)$ of $Sr_{4/3}(Mn_{2/3}Ni_{1/3})O_3$ to one formula unit.

The paramagnetic susceptibility curve $\chi_p(T)$ is written as

$$\chi_p(T) = \frac{C}{T}. \qquad [3a]$$

The susceptibility curve $\chi_{id}(T)$ for a mole of an isolated $(Mn^{4+})_2$ dimer is given by

$$\chi_{id}(T) = \frac{0.375g^2}{T} \times \frac{[2\exp(2J/k_BT) + 10\exp(6J/k_BT) + 28\exp(12J/k_BT)]}{[1 + 3\exp(2J/k_BT) + 5\exp(6J/k_BT) + 7\exp(12J/k_BT)]}, \qquad [3b]$$

where J is the spin exchange parameter between two Mn^{4+} ions. When the interdimer spin exchange interactions are treated in the molecular approximation (17), the susceptibility $\chi_d(T)$ can be written as

$$\chi_d = \frac{\chi_{id}}{1 - \left(\frac{2zJ'}{Ng^2\beta^2}\right)\chi_{id}}, \qquad [3c]$$

where J' is the spin exchange parameter for the interdimer interaction, and z is the number of nearest-neighbor dimers

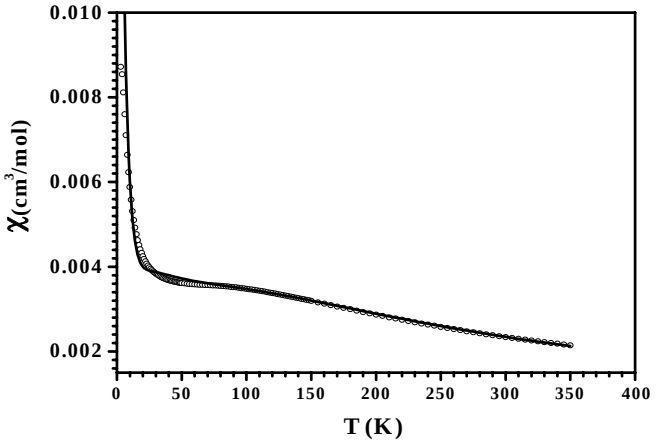

FIG. 5. Comparison of the experimental (empty circles) and calculated (solid line) magnetic susceptibilities of $Sr_{4/3}(Mn_{2/3}Ni_{1/3})O_3$.

interacting with a given dimer. Since the interchain interdimer interactions are expected to be much weaker than the intrachain interdimer interaction, the z value should be 2 in the present case.

In $Sr_{4/3}(Mn_{2/3}Ni_{1/3})O_3$ the $(Mn^{4+})_2$ dimers and the Ni^{2+} ions occur in a 1:1 ratio. All $(Mn^{4+})_2$ dimers should contribute equally to the magnetic susceptibility, while only about one-fifth of the Ni^{2+} ions (located at the TP centers) can, so that $y = \frac{5}{6}$. With $y = \frac{5}{6}$ and $z = 2$, the remaining parameters of Eq. [2] (i.e., J, J', and g for the Mn^{4+} ion lattice, and C for the Ni^{2+} ion lattice) can be determined by a least-square fitting of the $\chi_{exp}(T)$ curve with $\chi_{calc}(T)$. The solid line of Fig. 5 represents the $\chi_{calc}(T)$ curve thus obtained, and the fitting parameters are $J/k_B = -35.5$ K, $J'/k_B = -4.0$ K, $g = 1.96$, and $C = 1.06\ cm^3 \cdot K/mol$. Despite the simplicity of the TISS model, the overall fitting is surprisingly good ($R^2 = 0.9990$). It should be pointed out that the parameters derived from the fitting are consistent with the structural and physical properties of $Sr_{4/3}(Mn_{2/3}Ni_{1/3})O_3$. The number of unpaired spins, n, at each magnetic center of a paramagnetic system is related to the Curie constant C as $n(n+2) \approx 8C$. For Ni^{2+} ions located at the TP center, $n = 2$, so the C value should be approximately 1. This is indeed the case (i.e., $C = 1.06\ cm^3 \cdot K/mol$). The g value of 1.96 is also reasonable. The fitting shows that the intradimer and intrachain interdimer spin exchange interactions are both antiferromagnetic. This is consistent with the fact that $Sr_{4/3}(Mn_{2/3}Ni_{1/3})O_3$ exhibits a 3D antiferromagnetic ordering. In addition, the J value is larger than the J' value by an order of magnitude. This also agrees with the estimate from the spin dimer analysis that the intradimer interaction is considerably stronger than the intrachain interdimer interaction.

The observations that the TISS model reproduces the gross features of $\chi_{exp}(T)$, and that $Sr_{4/3}(Mn_{2/3}Ni_{1/3})O_3$ undergoes a 3D antiferromagnetic ordering at a low temperature, have important implications. The TISS model assumes that the Mn^{4+} ion and the Ni^{2+} ion sublattices are independent to a first approximation, namely, the spin exchange interaction of an $(Mn^{4+})_2$ dimer with its neighboring Ni^{2+} ions (when the latter has unpaired spins) are weak. $Sr_{4/3}(Mn_{2/3}Ni_{1/3})O_3$ undergoes a 3D antiferromagnetic ordering at a very low temperature. This ordering must take place in the Mn^{4+} ion sublattice, because an ordered arrangement of spin sites is present only in this sublattice. Thus, the interchain interdimer spin exchange interactions should be nonzero (though very small). The $Sr_{1.324}(Mn_{0.676}Ni_{0.324})O_3$ phase is close in structure to $Sr_{4/3}(Mn_{2/3}Ni_{1/3})O_3$, but contains a small amount of larger M_nO_{3n+3} octahedral oligomers ($n > 2$) in random fashion. Consequently, $Sr_{1.324}(Mn_{0.676}Ni_{0.324})O_3$ lacks an ordered arrangement of spin sites in the Mn^{4+} ion sublattice and is hence prevented from having a 3D antiferromagnetic ordering.

6. CONCLUDING REMARKS

The magnetic susceptibilities determined for two $Sr_{1+x}(Mn_{1-x}Ni_x)O_3$ phases with slightly different compositions ($x = \frac{1}{3}$ and 0.324) differ significantly, thus clearly pointing out the need for controlling phase compositions accurately in studying hexagonal perovskite-type oxides A_xMO_3. The temperature dependence of the magnetic susceptibility of $Sr_{4/3}(Mn_{2/3}Ni_{1/3})O_3$ is well reproduced by a simple model which assumes that the Mn^{4+} ion sublattice consists of weakly interacting antiferromagnetically coupled $(Mn^{4+})_2$ dimers, the Ni^{2+} ion sublattice has paramagnetic spins, and the two spin sublattices are independent. The success of this model indicates that the spin exchange interaction of an Mn^{4+} ion with its nearest-neighbor Ni^{2+} ion (located at the TP center) is weak.

ACKNOWLEDGMENTS

Work at North Carolina State University was supported by the Office of Basic Energy Sciences, Division of Materials Sciences, U.S. Department of Energy, under Grant DE-FG05-86ER45259.

REFERENCES

1. H. Fjellvåg, E. Gulbrandsen, S. Aasland, A. Olsen, and B. Hauback, *J. Solid State Chem.* **124,** 190 (1996).
2. J. A. Campá, E. Gutiérrez-Puebla, M. A. Monge, I. Raisines, and C. Ruiz-Valero, *J. Solid State Chem.* **108,** 230 (1994).
3. J. Darriet and M. A. Subramanian, *J. Mater. Chem.* **5,** 543 (1995).
4. W. T. A. Harrison, S. L. Hegwood, and A. J. Jacobson, *J. Chem. Soc., Chem. Commun.* 1953 (1995).
5. O. Gourdon, V. Petricek, M. Dusek, P. Bezdicka, S. Durovic, D. Gyepesova, and M. Evain, *Acta Crystallogr. B* **55,** 841 (1999).

6. A. El Abed, E. Gaudin, S. Lemaux, and J. Darriet, *Solid State Sci*., in press.
7. M. Evain, F. Boucher, O. Gourdon, V. Petricek, M. Dusek, and P. Bezdicka, *Chem. Mater*. **10,** 3068 (1998).
8. M.-H. Whangbo, H.-J. Koo, K.-S. Lee, O. Gourdon, M. Evain, S. Jobic, and R. Brec, *J. Solid State Chem*., in press.
9. R. Kriegel, A. Feltz, L. Walz, A. Simon, and H. J. Mattausch, *Z. Anorg Allg. Chem*. **99,** 617 (1992).
10. F. Illas, I. de P.R Moreira, C. de Graaf, and V. Barone, *Theor. Chem. Acc*. **104,** 265 (2000), and references cited therein.
11. D. Dai and M.-H. Whangbo, *J. Chem. Phys*. **114,** 2887 (2001).
12. A. Chartier, P. D'Arco, R. Dovesi, and V. R. Saunders, *Phys. Rev. B* **60,** 14042 (1999), and references cited therein.
13. H.-J. Koo and M.-H. Whangbo, *Inorg. Chem*. **40,** 2169 (2001), and references cited therein.
14. O. Kahn and B. Briat, *J. Chem. Soc*., *Faraday Trans*. 2 **72,** 268 (1976).
15. For a review, see: O. Kahn, "Molecular Magnetism," VCH Publishers, Weinheim, 1993.
16. H.-J. Koo, M.-H. Whangbo, S. Coste, and S. Jobic, *J. Solid State Chem*. **156,** 464 (2001), and the references cited therein.
17. A. P. Ginsberg and M. E. Lines, *Inorg. Chem*. **11,** 2289 (1972).